Sensors and Materials, Vol. 14, No. 7 (2002) 373–385
MYU Tokyo

S & M 0497

Structural and Ferroelectrical Properties of (111) Oriented Lead Zirconate Titanate Thick Films for Microultrasonic Sensors

Tsunehisa Tanaka, Xin-Shan Li[1], Arpporn Teeramongkonrasmee[2] and Yoshihiko Suzuki

Technology Research Institute of Osaka Prefecture, 2-7-1 Ayumino, Izumi City, Osaka 594-1157, Japan
[1]Seiko Epson Corporation, 80 Harashinden, Hirooka, Shiojiri City, Nagano 399-0785, Japan
[2]Department of Electrical Engineering, Chulalonkorn University, Payathai Rd., Patumwan, Bangkok 10330, Thailand

(Received December 14, 2001; accepted May 9, 2002)

Key words: PZT film, facing target sputtering, reactive sputtering

Lead zirconate titanate (PZT) thin films with highly oriented perovskite phase were prepared by two kinds of processes: (1) reactive DC sputtering with two facing metal targets, and (2) radio frequency (RF) sputtering with two facing PZT ceramic targets. The reactive DC sputtering deposition rate is 10 times as high as that of deposition by RF sputtering with ceramic targets. The 500°C-deposited film shows ferroelectric property with the values of remanent polarization (Pr) of 5.6 μC/cm^2 and saturation polarization (Ps) of 22.5 μC/cm^2. A multistep process was used for preparing (111) oriented PZT thick film with excellent properties by RF facing target sputtering. Suppression of cracks could be observed in PZT films with this multilayer structure. The XRD results showed that all films in the experiments showed a strong orientation of (111) perovskite phase. The polarization-electric field (P-E) hysteresis loops were improved with film thickness and Pr developed from 7 μC/cm^2 to 30 μC/cm^2, as film thickness increased from 0.24 to 4.6 μm. The dielectric constant also increased with film thickness, and reached the maximum value of 1300.

1. Introduction

PZT thin film is one of the best candidates for ultrasonic sensors because of its excellent piezoelectric properties. PZT films have been attracting extra attention recently.[1–5] In

order to achieve a thin film type ultrasonic sensor, a reliable technique for depositing thick PZT films is indispensable. Sensor performance depends strongly on the thickness of PZT film, and a high-sensitivity device can be obtained by increasing the film thickness to an optimal level. PZT thin films with highly oriented perovskite phase were prepared by two kinds of processes: (1) reactive DC sputtering with two facing metal targets, and (2) RF sputtering with PZT ceramic targets. It is very important for applications to micro-actuators or ultrasonic sensors to prepare highly oriented PZT thick films. The reactive DC sputtering with metal targets can be used for depositing thick film at a very high deposition rate. Therefore, we first attempted to use reactive DC sputtering, and then we attempted to use RF sputtering to prepare PZT film with excellent ferroelectric properties. It is very difficult to prepare PZT thick films with these properties by means of the conventional process, but the multistep method is suitable for preparing such PZT thick films with these properties. Highly (111) oriented perovskite PZT thick films with different thicknesses have been prepared by multistep processing. The multilayer PZT thick films are crack-free, and the surfaces are smooth. In order to control the orientation and grain growth of PZT thick film without cracks, one thin layer of PZT was deposited on the surface of the platinized silicon substrate by facing target sputtering, and then one or more thicker layers were deposited continuously until the needed thickness had been acquired, after the seeding layer was annealed at a higher temperature.

2. Experimental Procedures

All PZT films were deposited by facing target sputtering (FTS-1CB system, Osaka Vacuum Co.). Figure 1 shows the schematic diagram of the facing target sputtering system. The distance between targets was fixed at 100 mm and the distance between the substrate and the central line of the two targets was controlled at 135 mm. Two kinds of targets were used in this work: (1) an alloy plate of Zr/Ti(58%/42%), as well as a metal plate of Pb of the same size as the former was used for reactive DC sputtering, and (2) two hot-press sintered ceramic plates ($Pb_{1.2}$ $Zr_{0.58}$ $Ti_{0.42}$ O_x) with 100 mm diameter and 5 mm thickness were used for RF sputtering. Multilayers of Pt/Ti/SiO_2/Si were used as substrates for common sputtering and reactive sputtering, in which the thicknesses of the Pt, Ti and SiO_2 layers were 600, 30 and 800 nm, respectively.

The crystallographic characteristics of PZT films were determined by X-ray diffraction (XRD) analysis with Cu Kα radiation of 50 kV, 150 mA (Rigaku-RINT 2500). The micrographs of the surfaces of PZT films were obtained by scanning electron microscopy (SEM). The ferroelectric properties of PZT thin films were measured by an RT6000 system (Radiant Co.), in which the top electrodes were formed by depositing 0.2-mm-diameter Pt thin films on the surface of PZT thin film by magnetron RF sputtering at room temperature.

Table 1 summarizes the DC sputtering deposition conditions used in the experiments. PZT thin films were deposited with DC power from 100 to 600 W at substrate temperatures from 350 to 500°C.

Table 2 summarizes the RF sputtering deposition conditions used in the experiments. Each PZT layer was deposited at 300°C and 0.8 Pa under RF power 700 W.

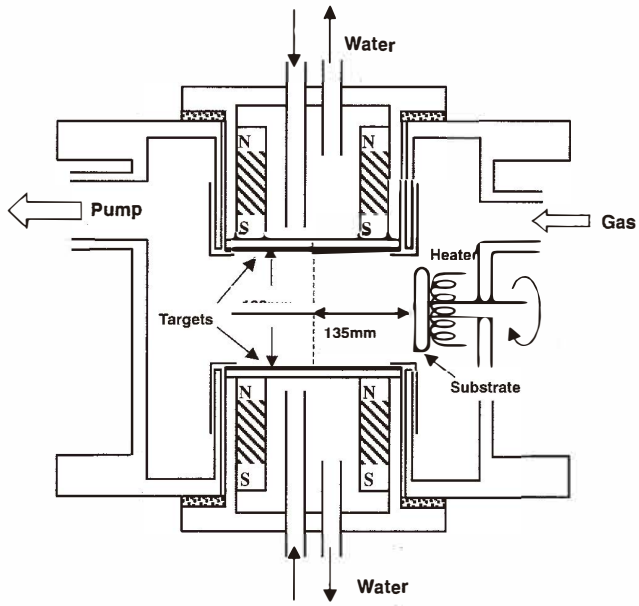

Fig. 1. Schematic diagram of the facing target sputtering system.

Table 1
Summary of DC sputtering deposition conditions.

Sputtering system	FTS-1CB (Osaka Vacuum)
Target composition	Pb, Zr/Ti (58%/42%) alloy
Substrate	Pt/Ti /SiO_2/Si
DC power	100–600 W
Substrate temperature	350–500˚C
Sputtering pressure	0.4 Pa
Sputtering O_2/Ar ratio	20:1

Table 2
Summary of RF sputtering deposition conditions.

Sputtering system	FTS-1CB (Osaka Vacuum)
Target composition	$Pb_{1.2}Zr_{0.58}Ti_{0.42}O_3$
Substrate	Pt/Ti /SiO_2/Si
RF power	700 W
Substrate temperature	300˚C
Sputtering pressure	0.8 Pa
Sputtering O_2/Ar ratio	2:1
Annealing temperature	600˚C in air
Heating rate	10˚C /min

The sample was transferred to a tube furnace and heated to 600°C in air with a heating rate of 30°C/min, before a further layer was deposited. A multistep process was used for preparing the PZT thick films. The sequence of this process is shown in Fig. 2.

X-ray diffraction spectra of the multilayer PZT films were taken with a Rigaku diffractrometer. The peak heights in the X-ray pattern were used to calculate a preferred oriented parameter, *e.g.*, $\alpha_{(111)} = I_{(111)}/I_{\text{Total}}$. To evaluate the electrical properties, top Al electrodes of 0.5 mm diameter were prepared by sputtering Al on a PZT surface, and patterned using a lift-off technique. Ferroelectric properties of all films were evaluated at a constant electric field of 170 kV/cm using a Radiant Technology ferroelectric tester, RT-6000, in the virtual ground mode for film thicknesses less than 1.5 μm. For thicker films, the polarization-electric field *(P-E)* hysteresis loops were measured using a high-voltage mode Sawyer-Tower circuit with a triangular wave at a frequency of 60 Hz. The low field dielectric constant, ε_r, was measured using a LCR meter for a field of 1.25 kV/cm at the frequency of 1 kHz.

3. Results and Discussion

3.1 *Reactive DC sputtering*

Figure 3 shows the deposition rate with increasing input DC power. When the input DC power increased from 100 W to 600 W, the deposition rate increased from 1.7 nm/min to 20.8 nm/min. This deposition rate is 10 times as high as that of deposition by RF sputtering with ceramic targets.

Figure 4 shows the XRD patterns of PZT films deposited by DC sputtering with an alloy Zr/Ti target and a metal Pb target. It is found that the phase composition of the film depends strongly on the substrate temperature. The pyrochlore phase disappears above 400°C, while the strong peaks of pyrochlore phase appear in the XRD pattern of a sample deposited at 350°C. There are only the peaks of perovskite phase and excess PbO_2 in the XRD patterns of samples deposited above 400°C. The sample deposited at 450°C shows a strong (111) peak of perovskite phase.

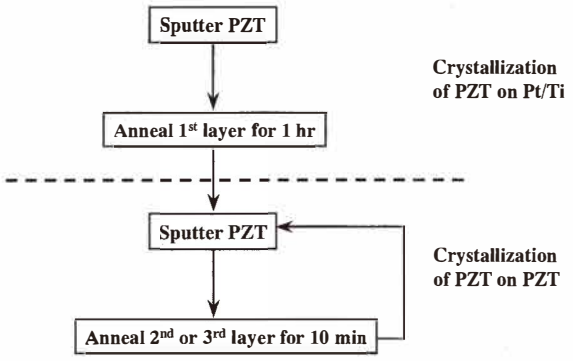

Fig. 2. Process flow used in the experiments.

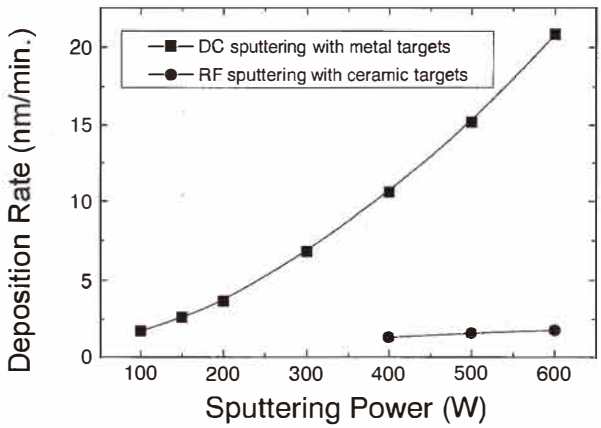

Fig. 3. Sputtering power dependence of deposition rate of PZT films deposited at 350°C.

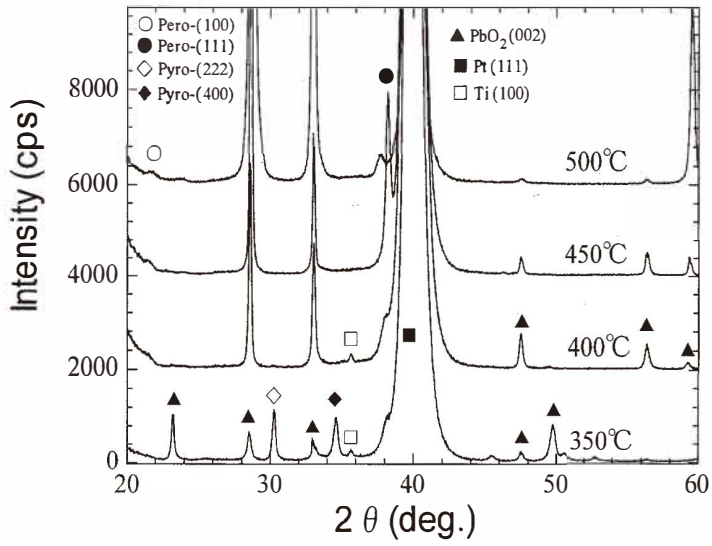

Fig. 4. XRD patterns of PZT thin films deposited by DC sputtering with facing metal targets at various temperatures under DC power of 200 W and 0.4 Pa in the ambient of O_2/Ar= 20 : 1.

The excess PbO_2 phase in the thin film samples can be reduced by modifying the target Pb with Zr and Ti blocks. When the areas of the Zr and Ti blocks are appropriate, the PZT thin film with single (111) perovskite phase can be obtained, excess ZrO_2 and TiO_2 phases

appear in the sample, and the target Pb is modified by Zr and Ti blocks which are too large. Figure 5 shows the XRD patterns of PZT thin films deposited at different temperatures by using modified target Pb with optimum area Zr and Ti blocks. It is found that only perovskite phase can be detected although peaks from the substrate are included in the figure. Even if the substrate temperature is as low as 350°C, the peak of pyrochlore phase does not appear. In particular, the sample deposited at 500°C shows a very strong (111) peak of perovskite phase. This indicates that reactive facing target sputtering is suitable for preparing perovskite PZT thin films.

Figure 6 shows the hysteresis loops of reactive sputtered PZT thin films. It is found that the ferroelectric properties of all samples depend strongly on the deposition temperature. It is evident from Fig. 5 that *Pr* and *Ps* of the reactive sputtered sample increase with the increase of deposition temperature. The 500°C-deposited film shows ferroelectric property with *Pr* of 5.6 μC/cm^2 and *Ps* of 22.5 μC/cm^2. These low *Pr* and *Ps* may be caused by the leakage current of the film.

3.2 *RF sputtering*

Figure 7 shows the XRD patterns of PZT thin films deposited by RF sputtering with ceramic targets and successively annealed at 600°C. It is found that there are almost no other peaks except for that of (111) oriented perovskite phase in the samples deposited in the range from 285°C to 435°C. However, other peaks of perovskite phase such as (100),

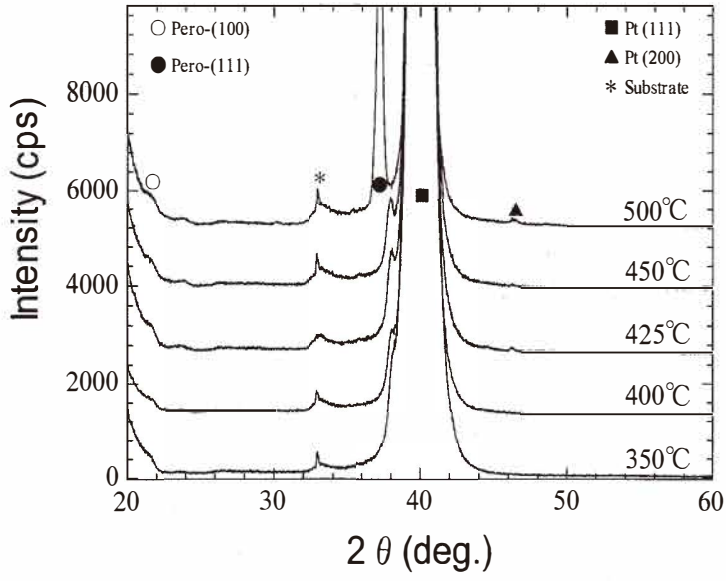

Fig. 5. XRD patterns of PZT thin films deposited at various temperatures under DC power of 400 W, 0.4 Pa in the ambient of O_2/Ar= 20 : 1 by using modified target Pb with optimum area Zr and Ti blocks.

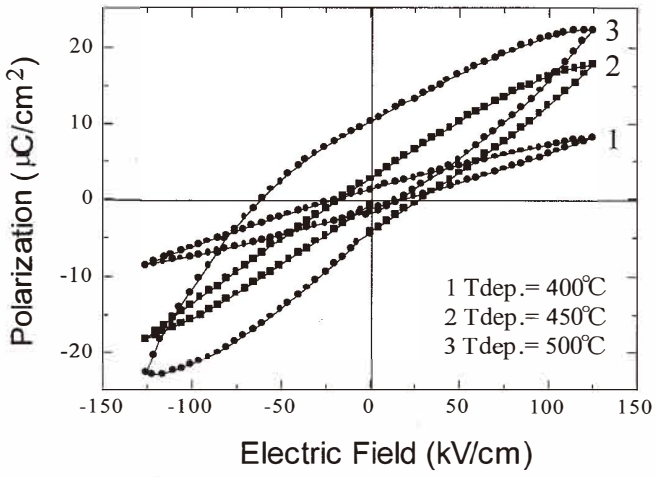

Fig. 6. Hysteresis loops of reactive DC sputtered PZT films.

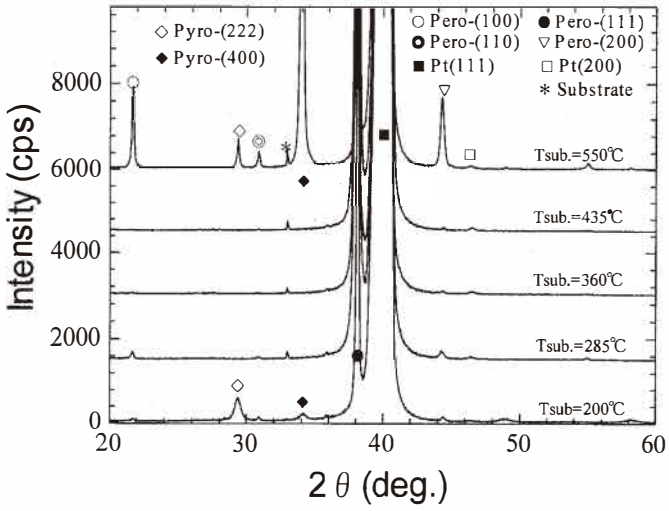

Fig. 7. XRD patterns of PZT thin films deposited at various temperatures under RF power of 700 W.

(110) and (200) peaks as well as the strong peaks of pyrochlore phase, exist in the sample deposited at 550°C. In the case of the samples deposited at very low substrate temperatures, the peak of (222) pyrochlore phase appears in the XRD pattern. This indicates that too high or too low a deposition temperature is not advantageous for the formation of (111)

oriented perovskite phase in the annealed PZT thin films. Meanwhile, the crystallization process of PZT thin film is found to depend strongly on the annealing temperature. There is almost only (111) oriented perovskite phase in the 600°C-annealed sample which was deposited in the range of 285–435°C. More and more other phases such as pyrochlore phase and lead oxide phase appear in the samples annealed at lower temperatures. Good ferroelectric characteristics were obtained in the RF sputtered films.

3.3 *Multistep process*

Figure 8 shows XRD patterns of the films prepared with the multistep process. All films show the strong texture of (111) orientation. Figure 9 shows the preferred orientation parameter of (111) orientation, which is defined in section 2, as a function of film thickness. Two kinds of processes are compared in Fig. 9. It is evident from Fig. 8 and Fig. 9 that all multilayer films exhibit the strong texture of (111) orientation with $\alpha_{(111)}$ greater than 97% at varied film thicknesses. However, in the case of single-layer and two-layer films, (111) orientation decreases with film thickness (Fig. 9). This indicates that the surface of every annealed layer in the thick film can also serve as a nucleation site for the (111) perovskite phase of PZT,[7,8] even if the multilayer film is as thick as 6 μm.

The improvement of surface morphology can be observed in multilayer PZT films (Fig. 10a, b). The surfaces of the multilayer films are smooth and crack-free. The average grain size is 50–100 nm. The SEM cross-section of the six-layer PZT film is shown in Fig.10(c). Its fracture reveals individual layers. The improvement in surface roughness apparently resulted in a film with a better degree of orientation.[9]

The ferroelectric characteristics are shown in Fig. 11. The *P-E* hysteresis loop for the 0.24-μm-thick film is broad, inclined and shifted along the positive electric field axis. The

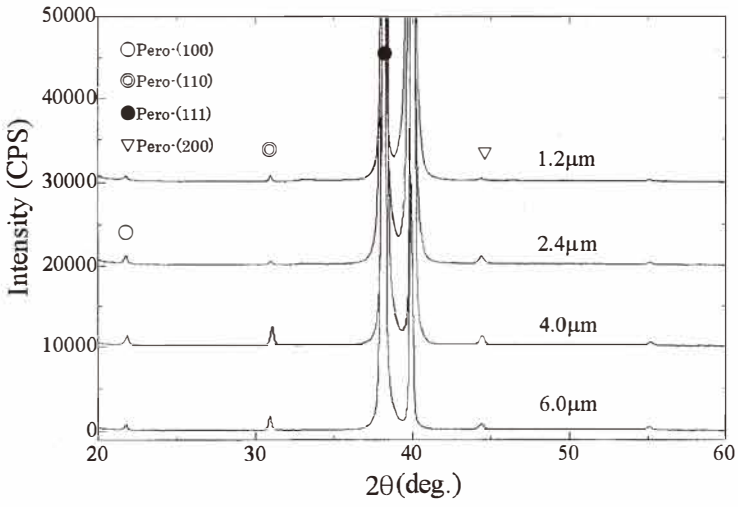

Fig. 8. XRD spectra of multilayer PZT films.

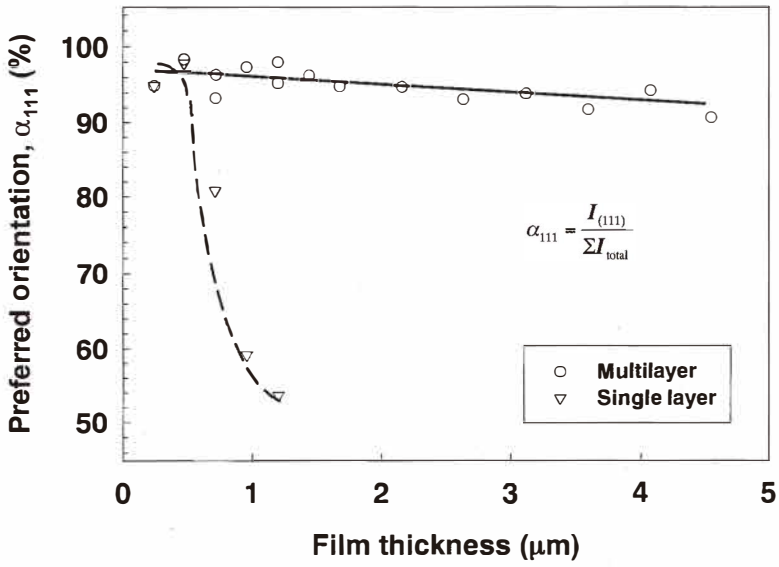

Fig. 9. (111) preferred orientation as a function of film thickness in the cases of single-layer and multilayer films.

shift along the electric field axis is consistent with a significant internal bias field in our samples.[10] But as the thickness increased the shift became smaller, and the loops became squarer and more saturated. Values of *Ps* and *Pr* are plotted versus film thickness in Fig. 11(a). Both *Ps* and *Pr* are improved with film thickness. The values of *Pr* varied from 7 μC/cm^2 for a 0.24 μm film to 30 μC/cm^2 for a 4.6 μm film. The coercive field *Ec* also showed strong dependence on the field thickness as shown in Fig. 11(b). The values of *Ec* decreased sharply for the films below 1–2 μm film, and are expected to reach the value of 20 kV/cm for thicker films.

The dielectric constant of multilayer films is shown in Fig. 12(a). It increases from 700 to 1300 with the increase of film thickness from 0.24 to 2 μm, and then the dielectric constant almost retains a constant when the thickness is more than 2 μm.

The effects of PZT film thickness on dielectric and ferroelectric properties are interpreted as being due to the proportionately greater contribution from the interfacial effect as the sample thickness decreased.[11,12] To demonstrate the dependence of the dielectric constant on film thickness, the reciprocal of small signal capacitance was plotted with film thickness. A linear relation with a nonzero interception was obtained. The nonzero interception indicates the existence of non-ferroelectric capacitance at the interface between our PZT film and the electrode. We can interpret the equivalent circuit of our PZT film as a series connection of ferroelectric capacitance and non-ferroelectric capacitance. The mathematical model for this equivalent circuit can be described as follows:

$$\frac{1}{C_{\text{meas}}} = \frac{1}{C_0} + \frac{1}{C_{\text{ferro}}} = \frac{1}{C_0} + \frac{d}{A\varepsilon_0\varepsilon_r},$$

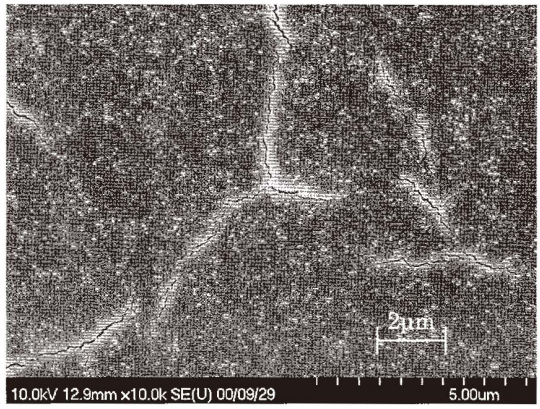

(a) Single-layer PZT film

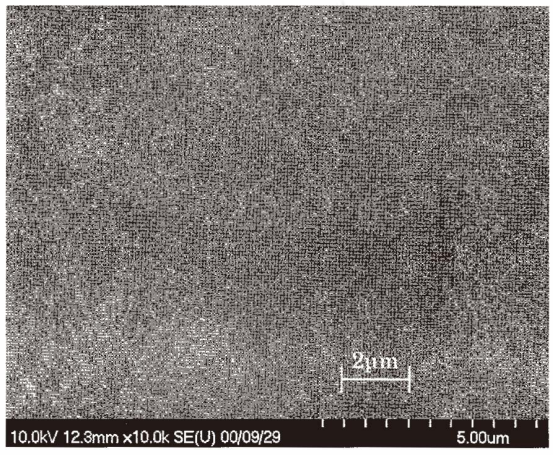

(b) Multilayer PZT film

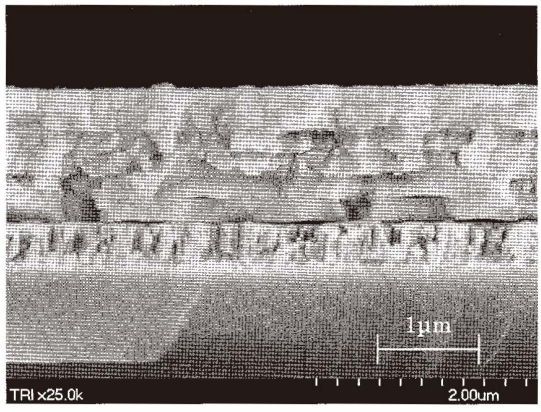

(c) Cross-section of a six-layer PZT film

Fig. 10. Comparison of surface morphology for 1.2 μm.

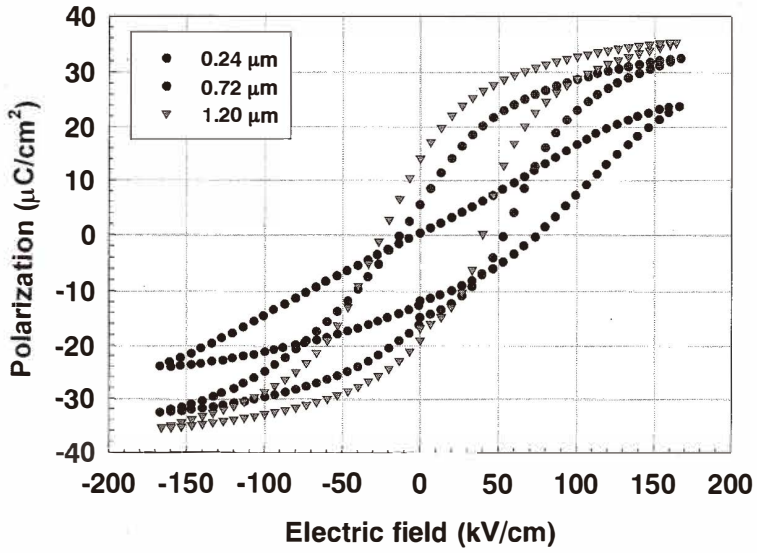

(a)

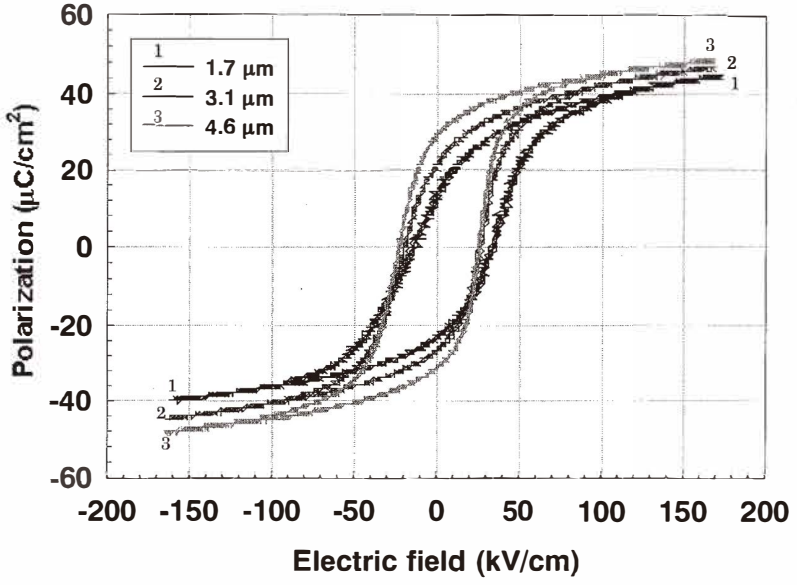

(b)

Fig. 11. P-E hysteresis loops for (a) 0.24-, 0.72- and 1.2-μm-thick and (b) 1.7-, 3.1- and 4.6-μm thick multilayer PZT films.

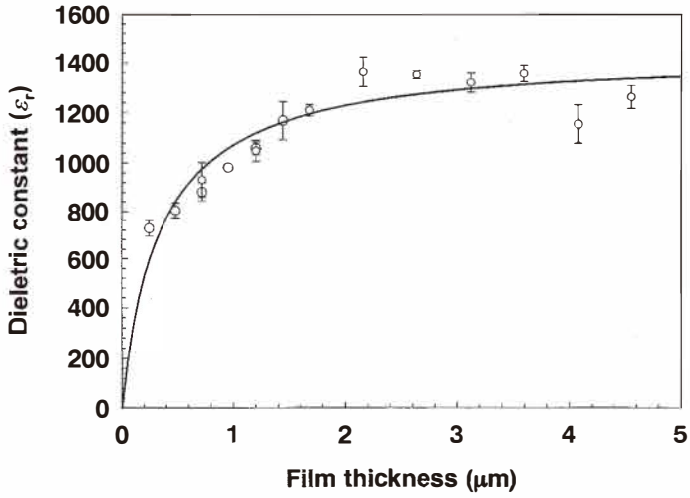

(a)

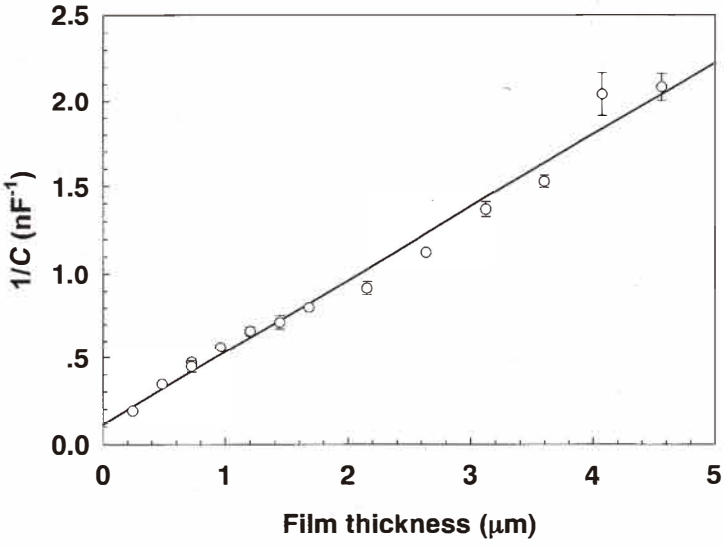

(b)

Fig. 12. (a) Dielectric constant and (b) reciprocal of capacitance as a function of film thickness.

where d is the film thickness, A is the top electrode area and ε_0 and ε_r are the permittivity of free space and the dielectric constant of PZT, respectively. With this model, we can calculate the dielectric constant of the pure ferroelectric phase to be approximately 1400. The variations of the dielectric constant with film thickness were calculated using this value. The variations of the dielectric constant with film thickness were calculated using this value as shown by the solid line in Fig.12(b). The agreement between the calculated curve and the experimental data was fairly good. This mean is due to the existence of the degraded interface layer in the film.

4. Conclusions

The reactive DC sputtering of deposition rate increases from 1.7 nm/min to 20.8 nm/min. This deposition rate is 10 times as high as that of deposition by RF sputtering with ceramic targets. It is found that the *Pr* and *Ps* of reactive sputtered samples increase with the increase of deposition temperature. The 500°C-deposited film shows ferroelectric property with *Pr* of 5.6 μC/cm^2 and *Ps* of 22.5 μC/cm^2.

Highly oriented (111) PZT films of up to 4.6 μm thickness were prepared by the multistep process. The suppression of cracks could be observed in PZT films with the multilayer structure. The XRD results showed that all films in the experiments showed a strong orientation of (111) perovskite phase. Under a constant electric field measurement, *P-E* loops improved with film thickness and remanent polarization, and *Pr* developed from 7 μC/cm^2 to 30 μC/cm^2, when film thickness increased from 0.24 to 4.6 μm. The dielectric constant also increased with film thickness, and reached the maximum value of 1300. The variations are interpreted in terms of the influence of the interfacial layer on the electrical characteristics.

References

1 H. D. Chen, K. R. Udayaumar, C. J. Gaskey and L. E. Cross: J. Am. Ceram. Soc. **79**(1996) 2189.
2 J. J. Bernstein, S. L. Finberg, K. Houston, L. C. Niles, H. D. Chen, L. E. Cross, K. K. Li and K. Udayakumar: IEEE Trans. Ultranson., Ferroelect., Freq. Contr. **44** (1997) p. 960.
3 H. J. June and T. S. Kim: J. Appl. Phys. **79** (1996) 9245.
4 K. Sreenivas, M. Sayer and P. Garrett: Thin Solid Films **172** (1989) 251.
5 T. Kijima: Extended Abstracts (The 47th Spring Meeting 2000), The Japan Society of Applied Physics and Related Societies, No. 0, 11.
6 X. S. Li, T. Tanaka and Y. Suzuki: J. Vac. Soc. Jpn. **42** (1999) 257.
7 R. Kurchania and S. J. Milne: J. Mater. Res. **14** (1999) 1852.
8 K. Maki, N. Soyama, S.Mori and K. Ogi: Jpn. J. Appl. Phys. **39** (2000) 5421.
9 B. A. Tuttle, J. A. Voigt, D. C. Goodnow, D. L. Lamppa, T. J. Headly, M. O. Eatough, G. Zender, R. D. Nasby and S. M. Roders: J. Am. Ceram. Soc. **76** (1993) 537.
10 G. E. Pike, W. L. Warren, D. Dimos, B. A. Tuttle, R. Ramesh, J. Lee, V. G. Keramids and J. T. Evans, Jr: Appl. Phys. Lett. **66** (1995) 484.
11 K. Amanuma, T. Moori, T. Hase, T. Sakuma, A. Ochi and Y. Miyasaka: Jpn. J. Appl. Phys. **32** (1993) 4150.
12 P. K. Larsen, G. J. M. Dormas, D. J. Taylor and P. J. Van Veldhoven: J. Appl. Phys. **76** (1994) 2405.